

Viscous damping of microresonators for gas composition analysis

Yang Xu

Department of Mechanical Engineering, University of Louisville, Louisville, Kentucky 40292

J.-T. Lin and Bruce W. Alphenaar

Department of Electrical and Computer Engineering, University of Louisville, Louisville, Kentucky 40292

Robert S. Keynton^{a)}

Department of Bioengineering and Department of Mechanical Engineering, University of Louisville, Louisville, Kentucky 40292

(Received 20 November 2005; accepted 22 February 2006; published online 7 April 2006)

The damping effect of various gas environments on a silicon, lateral microresonator implemented with piezoresistive detection is investigated in this study. The resonant frequency of the cantilever shifts due to viscous damping by an amount that is directly determined by the molar mass of the gas, thereby providing a method to determine the composition of the gas environment. In addition, the microresonator demonstrates the ability to perform CO₂ composition analysis using this nonreaction based detection method. The advantages of this gas analysis method are that it is simple, repeatable, reversible and not limited to reactive gases. © 2006 American Institute of Physics. [DOI: 10.1063/1.2193347]

The high resonance frequency, high quality factor and small dimensions of micro and nano resonators have led to their consideration for a variety of gas sensing applications. Micro/nano resonator gas sensors detect the shift in resonance frequency that occurs when the cantilever mass or surface stress changes due to interactions with gas particles.¹⁻³ This detection method requires a chemical reaction between the sensed gas and the resonator, such as adsorption or desorption of gas particles or intercalation of gas into the cantilever lattice. The usefulness of microresonator gas sensors is limited by the availability of suitable gas reaction mechanisms, and by the irreversibility of the detection process. There is also a sizable, nonchemical interaction of the microresonator with the gaseous environment, via the damping force of the gas particles on the cantilever. This restricts the operation of reaction-based microresonator gas sensors to near vacuum conditions. While this limitation is generally recognized, overlooked is the fact that this same damping force can itself be used as a means of nonreactive gas sensing. In 1992, Blom *et al.*⁴ calculated the shift in resonance frequency of a microcantilever due to the damping effect, and demonstrated that the shift is a function of molar mass and gas pressure. By measuring the resonance frequency shift due to the damping effect, the molar mass of the gas can be obtained, and the gas or the composition of the gases in the environment can be determined.

Here, we demonstrate the use of the damping force for gas sensing in a lateral silicon microresonator. The amplitude of the resonance signal and the resonance frequency are both shown to be systematically dependent on the molar mass of the gas environment at a fixed pressure, which provides a viable method for gas identification without involving reactions between the gas and resonator. The device developed in this study can be operated at atmospheric pressure and uses piezoresistive sensing,⁵⁻⁸ so that cumbersome optical components are not required for resonance detection. The damp-

ing force detection method can be used for sensing inert gases, measuring the composition of binary gas mixtures or monitoring changes in the environment as a function of time. Although this technique is not suitable for detecting small quantities of gas, it is simple, repeatable and reliable compared to reaction-based detection methods and provides a means to sense nonreactive gases.

Blom *et al.*⁴ theoretically analyzed the effect of damping in a gaseous environment on the resonance frequency and quality factor of microresonators. Three regimes were described to account for the change in the resonance frequency with increasing pressure: the intrinsic, molecular, and viscous regimes. At low pressure, within the intrinsic and molecular regimes, the resonance frequency shift due to damping force is negligible. At higher pressure, in the viscous regime, the inertial force of the gas on the resonator creates a damping effect, which lowers the resonance frequency. The relative resonance frequency shift in the viscous regime is given by

$$\Delta f/f = \frac{\pi R^3}{3m_b R_0 T} \left(MP + \frac{9}{2} \frac{\sqrt{\mu R_0 T / \pi f}}{R} \sqrt{MP} \right),$$

where m_b is the mass of the cantilever, $R_0 = 8.314 \text{ J mol}^{-1} \text{ K}^{-1}$ is the gas constant, T is the absolute temperature, M is the molar mass of the gas, P is the pressure, μ is the dynamic viscosity of the gas, f is the resonance frequency in vacuum and Δf is the shift of the resonance frequency.⁴ To derive this formula, the cantilever is approximated by a string of spheres,^{4,9} with R being the radius of one of the spheres. The inertial force of the gas is proportional to the product of the mass times the acceleration of the gas in contact with the cantilever. The relative resonance frequency shift due to inertial damping is thus dependent on the molar mass of the gas in the environment. By measuring the relative resonance frequency shift at a specific temperature and pressure (e.g., room temperature and atmospheric pressure), the molar mass of the unknown gas can be obtained.

^{a)} Author to whom correspondence should be addressed; electronic mail: rob.keynton@louisville.edu

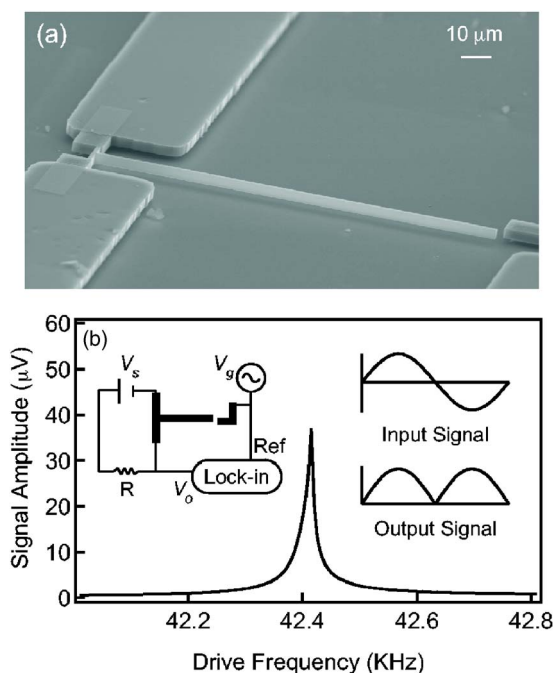


FIG. 1. (a) SEM image of the lateral vibration T-shaped microresonator. The free end of the resonator is approximately $2 \mu\text{m}$ away from the driving electrode. The width and the height of the resonator are 1.1 and $3 \mu\text{m}$, respectively, and the lengths are $9 \mu\text{m}$ for the base of the T-shaped resonator and $127 \mu\text{m}$ for the cantilever extending from the base. (b) Resonance curve obtained from the measurement of the output voltage V_o as a function of the frequency of the gate voltage V_g . The amplitudes of V_s and V_g are both set at 5 V . Left inset: measurement circuit used for piezoresistive detection. Right inset: schematic drawing showing the relationship between the input and output signals.

Figure 1(a) shows a scanning electron microscope (SEM) image of the lateral vibration silicon resonator used in our study. A T-shaped resonator is defined from the top silicon layer of a silicon-on-insulator wafer using electron beam lithography and deep-reactive-ion etching (DRIE). For DRIE, a C_4H_8 etching process with a simultaneous SF_6 passivation process is performed to obtain smooth sidewalls. The resonator is released through wet etching of the underlying silicon dioxide layer, followed by critical point drying. As shown in Fig. 1(b), the base of the resonator is fixed at both ends by electrical contacts and acts as a piezoresistive sensing element. The cantilever beam extends from the base and is driven by a capacitively coupled gate electrode.

Microresonator characterization was done in a probe station with a variable pressure sample chamber. The cantilever is driven electrostatically by applying an ac bias, V_g , to the gate electrode, and sweeping the drive frequency, f_A , around the resonance frequency, f . A dc bias, V_s , is applied across the base in series with a $1 \text{ k}\Omega$ resistor, R [left inset of Fig. 1(b)]. Movement of the cantilever applies stress to the base, and results in an increase in resistance along its length. This produces an ac output voltage V_o , which is monitored using a lock-in amplifier. As shown in the right inset to Fig. 1(b), vibration of the cantilever at a frequency f_A produces a voltage signal of frequency $2f_A$. The doubling of frequency occurs because motion of the cantilever in either the left or right direction results in an equivalent increase in the resistance of the base. Figure 1(b) shows a typical response curve of the resonator using the piezoresistive detection method at a pressure of 10^{-2} Torr in air environment. A sharp peak is observed in V_o as a function of f_A , demonstrating that the

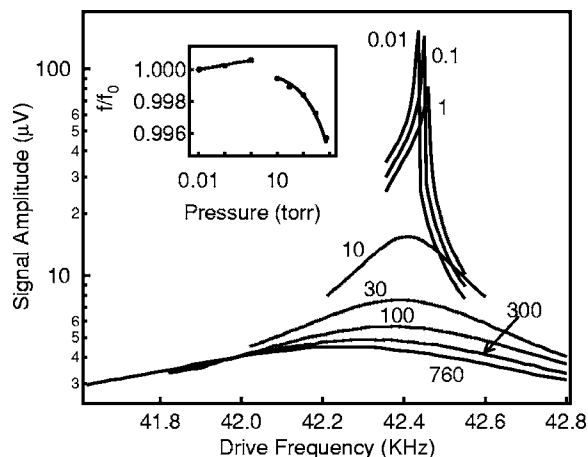


FIG. 2. Resonance frequency response curves of a T-shaped resonator for pressures of 0.01 , 0.1 , 1 , 10 , 30 , 100 , 300 , and 760 Torr in a methane environment. Inset: relationship between relative resonance frequency and pressure for a methane environment.

resonance frequency of this cantilever is 42.41 KHz with a quality factor of 2170 . The resonator response was also characterized in a SEM to prove that the peak in V_o correlated with the peak amplitude of the cantilever oscillations.

Figure 2 shows the resonance curves of the cantilever in a methane environment with pressures of 0.01 , 0.1 , 1 , 10 , 30 , 100 , 300 , and 760 Torr. As shown in the inset, the resonance frequency increases a small amount as the pressure increases from 0.01 to 1 Torr and then falls as the pressure increases from 1 Torr to atmospheric pressure. The increase in resonance frequency in the low pressure regime has not been reported in resonators using an optical detection method,^{10,11} suggesting that it is related to our piezoresistive detection technique. Piezoresistive sensing requires current to flow through the base of the cantilever, which is expected to raise the resonator temperature somewhat due to Joule heating. As the pressure increases, the excess heat dissipates more easily through the gaseous environment, lowering the temperature of the cantilever relative to its temperature in vacuum. The resonant frequency of microcantilevers has been found to increase with decreasing temperature due to the increase in Young's modulus,¹²⁻¹⁴ which can account for the increase in the resonance frequency that we observe.

Of primary interest is the regime above 1 Torr, in which the resonance frequency is observed to decrease substantially. This is the viscous damping regime where the resonance frequency shift is due to the inertial force of the gas on the cantilever. A fit of our data in the viscous damping regime to Eq. (1) is shown in Fig. 2, using R as the sole "fitting" parameter. The data fit the theory very well using a value of $R=5.27 \mu\text{m}$. The difference in this value from the average half width of our cantilever is, most likely, due to the influence that the cantilever geometry has on the resonant frequency shift compared with the string-of-spheres model employed in Ref. 4. In Fig. 3, the shift in resonance frequency in the viscous damping regime is plotted as a function of pressure for four different gases: helium, methane, nitrogen and argon, with molar masses of 4 , 16 , 28 and 40 g/mol , respectively. The results indicate a clear dependence of the resonance frequency shift on the molar mass of the gas. As predicted by theory, the frequency shift is observed to increase as the molar mass increases. For each gas, we can analyze our results using Eq. (1) above. The curve

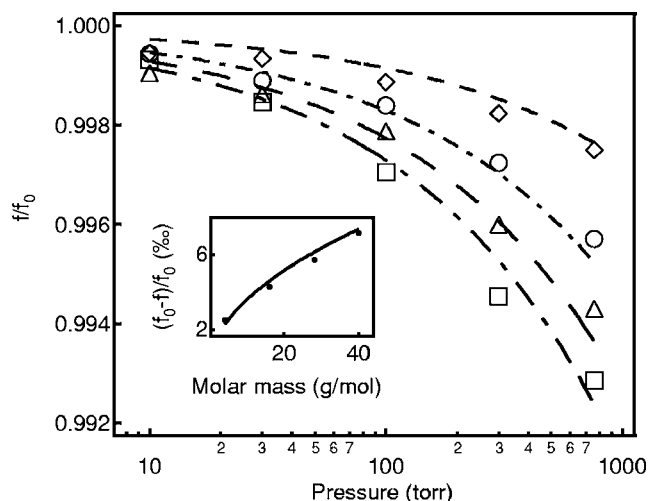


FIG. 3. The relative resonance frequency as a function of pressure from 10 to 760 Torr in helium (\diamond), methane (\circ), nitrogen (\triangle), and argon (\square) environments. Inset: the relative resonance frequency shift of a resonator for the four gases at atmospheric pressure.

fits shown in Fig. 3 are each done using a single value for the fitting coefficient of $R=5.4 \mu\text{m}$. Although the dynamic viscosities of the four gases vary between $\mu=1.1 \times 10^{-5}$ and $\mu=2.217 \times 10^{-5}$ NS/m², a single value of $\mu=2 \times 10^{-5}$ NS/m² is used to simplify the curve fitting process. The resonance frequency shift is only weakly dependent on the dynamic viscosity, and its exact value does not appreciably influence the curve fit.

For the resonator to function as a gas sensor, it must be possible to extract the molar mass from the resonance frequency shift. In the inset to Fig. 3, the relative resonance frequency shift is plotted as a function of the molar mass of the gas at a pressure of 760 Torr. The resonant frequency shift changes from 0.25% (or 2.5‰) to 0.71% (or 7.1‰) as the molar mass increases from 4 to 40 g/mol, respectively. A curve fit to Eq. (1) using the same value of $R=5.4 \mu\text{m}$ is also provided. The four experimental points lie on this curve to within an average deviation of ± 2 g/mol. While this accuracy is clearly not suitable for precision gas analysis, the sensor could find application in determining changes in normal ambient conditions due to the introduction of contaminant gases. To demonstrate this capability, we performed measurements on the resonance frequency shift as a function of CO₂ concentration in air at room temperature and atmospheric pressure. The results of these measurements are shown in Fig. 4. As the CO₂ concentration increases, the resonance frequency shift also increases, as would be expected due to the increase in the molar mass of the ambient environment. A 20% change in the CO₂ concentration results in a 0.05% (or 0.5‰) change in the resonant frequency, corresponding to a frequency change of 20 Hz. The sensitivity can be improved by decreasing the length of the cantilever, since, according to Eq. (1), the relative frequency shift is inversely proportional to the mass and hence to the length of the cantilever. It should be noted that temperature and humidity of the environment also influence the resonance frequency of the microresonator. Specifically, changes in the

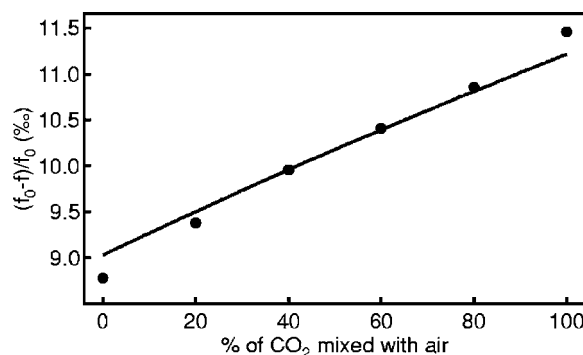


FIG. 4. Relative resonance frequency shift of the resonator as a function of the percent CO₂ in an air/CO₂ mixture at atmospheric pressure.

environmental temperature will alter both the resonator temperature and the resistance of the piezoresistive sensor, which will result in a resonance frequency shift and a change in signal amplitude, respectively. Humidity variations, on the other hand, will alter the molar mass of the environment which will directly influence the resonance frequency of the microresonator. Thus, these factors need to be carefully controlled during sensor operation.

In summary, we have demonstrated the influence of gases with different molar mass on the resonance frequency of a lateral vibrating silicon resonator in the viscous damping regime. We also illustrate the potential of a microresonator gas sensor based on the viscous damping force. The fabrication of the resonator is simple and the operation of the device is easy, reliable and repeatable. Because the detection method has a nonchemical basis, gas sensing is not limited by the availability of reaction mechanisms.

The authors thank Professor Tim Dowling for providing the original motivation for this work and Mehdi Yazdanpanah for useful discussions. Funding provided by NSF/ONR (No. ECS-0224114), NSF (No. EPS-0447479), NSF-EPSCOR (No. 6016955) and DOE-EPSCOR (No. 46411101095).

¹T. Thundat, E. A. Wachter, S. L. Sharp, and R. J. Warmack, *Appl. Phys. Lett.* **66**, 1695 (1995).

²P. G. Datskos and I. Sauer, *Sens. Actuators B* **61**, 75 (1999).

³X. M. H. Huang, M. Manolidis, S. C. Jun, and J. Hone, *Appl. Phys. Lett.* **86**, 143104 (2005).

⁴F. R. Blom, S. Bouwstra, M. Elwenspoek, and J. H. J. Fluitman, *J. Vac. Sci. Technol. B* **10**, 19 (1992).

⁵M. Tortorese, R. C. Barrett, and C. F. Quate, *Appl. Phys. Lett.* **62**, 834 (1993).

⁶J. A. Harley and T. W. Kenny, *Appl. Phys. Lett.* **75**, 289 (1999).

⁷I. Bargatin, E. B. Myers, J. Arlett, B. Gudlewski, and M. L. Roukes, *Appl. Phys. Lett.* **86**, 133109 (2005).

⁸M. Gel and I. Shimoyama, *J. Micromech. Microeng.* **14**, 423 (2004).

⁹K. Kokubun, M. Hirata, H. Murakami, Y. Toda, and M. Ono, *Vacuum* **34**, 731 (1984).

¹⁰R. Sandberg, W. Svendsen, K. Molhave, and A. Boisen, *J. Micromech. Microeng.* **15**, 1454 (2005).

¹¹S. J. O'Shea, P. Lu, F. Shen, P. Neuzil, and Q. X. Zhang, *Nanotechnology* **16**, 602 (2005).

¹²X. Li, T. Ono, Y. Wang, and M. Esashi, *Appl. Phys. Lett.* **83**, 3081 (2003).

¹³U. Gysin, S. Rast, P. Ruff, E. Meyer, D. W. Lee, P. Vettiger, and C. Gerber, *Phys. Rev. B* **69**, 045403 (2004).

¹⁴J. Han, C. Zhu, J. Liu, and Y. He, *Sens. Actuators, A* **101**, 37 (2002).